



Final Draft of the original manuscript

Zimmermann, T.; Mohammed, F.; Reese, A.; Wieser, M.; Kleeberg, U.; Pröfrock, D.; Irrgeher, J.:

Zinc isotopic variation of water and surface sediments from the German Elbe River.

In: Science of the Total Environment. Vol. 707 (2020) 135219.

First published online by Elsevier: 22.11.2019

<https://dx.doi.org/10.1016/j.scitotenv.2019.135219>

1
2
3
4
5
6
7
8
9
10
11
12
13
14
15
16
17
18
19
20
21
22
23
24

Zinc isotopic variation of water and surface sediments from the German Elbe River

Zimmermann T.^{1, 2}, Mohamed A. F.³, Reese A.^{1, 2}, Wieser M. E.³, Kleeberg U.¹, Pröfrock, D.^{1,*}, Irrgeher, J.^{1,3#}

*corresponding author

Daniel Pröfrock (daniel.proefrock@hzg.de, phone +49415287-2846)

¹ Helmholtz-Zentrum Geesthacht, Institute of Coastal Research, Marine Bioanalytical Chemistry, Max-Planck Str. 1, 21502 Geesthacht, Germany

² Universität Hamburg, Department of Chemistry, Inorganic and Applied Chemistry, Martin-Luther-King-Platz 6, 20146 Hamburg, Germany

³ University of Calgary, Department of Physics and Astronomy, 2500 University Drive NW, Calgary, Alberta T2N 1N4, Canada

#present address: Montanuniversität Leoben, Department of General, Analytical and Physical Chemistry, Chair of General and Analytical Chemistry, Franz Josef-Straße 18, 8700 Leoben, Austria

Abstract

Recent studies suggested the use of the isotopic composition of Zn as a possible tracer for anthropogenic Zn emissions. Nevertheless, studies mainly focused on sampling areas of a few

25 km² with well-characterized anthropogenic Zn emissions. In contrast, this study focused on
26 analyzing a large sample set of water and sediment samples taken throughout the course of the
27 Elbe River, a large, anthropogenically impacted river system located in Central Europe. The
28 primary objective was to evaluate the use of the isotopic composition of Zn to trace
29 anthropogenic Zn emission on a large regional scale. In total 19 water and 26 surface sediment
30 samples were investigated, covering the complete course of over 700 km of the German Elbe
31 between the German/Czech border and the German North Sea, including six tributaries. Stable
32 isotope abundance ratios of Zn were assessed by multi-collector inductively coupled plasma
33 mass spectrometry (MC ICP-MS) in water filtrates (<0.45 μm) and total digests of the sieved
34 surface sediment fraction (<63 μm) after analyte/matrix separation using Bio-Rad AG MP-1
35 resin via a micro-column approach and application of a ⁶⁴Zn/⁶⁷Zn double spike. Measured
36 isotopic compositions of $\delta^{66}\text{Zn}/^{64}\text{Zn}_{\text{IRMM-3702}}$ ranged from -0.1 ‰ to 0.3 ‰ for sediment
37 samples, and from -0.5 ‰ to 0.4 ‰ for water samples. In comparison to historical data some
38 tributaries still feature high mass fractions of anthropogenic Zn (e.g. Mulde, Triebisch)
39 combined with $\delta^{66}\text{Zn}/^{64}\text{Zn}_{\text{IRMM-3702}}$ values higher than the lithogenic background. The
40 dissolved $\delta^{66}\text{Zn}/^{64}\text{Zn}_{\text{IRMM-3702}}$ values showed a potential correlation with pH. Our results
41 indicate that biogeochemical processes like absorption may play a key role in natural Zn
42 isotopic fractionation making it difficult to distinguish between natural and anthropogenic
43 processes.

44

45 **Keywords**

46 MC ICP-MS, Zn double spike, isotope tracer, environment, isotopic fractionation, metal
47 pollution

48 **1 Introduction**

49 The analysis of Zn isotope ratios is a rather new field of non-traditional stable isotope analysis.
50 It was not until the early 2000s that significant natural variations in isotopic composition of Zn
51 were reported, even though the first work on Zn isotopic composition based on thermal
52 ionization mass spectrometry (TIMS) dates back to the mid-1950s (Blix et al., 1957). Pioneer
53 work using multi-collector inductively coupled plasma mass spectrometry (MC ICP-MS) was
54 done by Maréchal et al. (1999) who, for the first time, reported significant natural variation in
55 Zn isotopic composition. Further early work covered the analysis of ferromanganese nodules
56 and ocean sediment (Maréchal et al., 2000), deep sea carbonates (Pichat et al., 2003) or higher
57 plants (Weiss et al., 2005).

58 Since the natural variation of the Zn isotopic composition is rather small (ca. 1 – 2 ‰) (Brand
59 et al., 2014), significant effort had to be put into optimizing MC ICP-MS sample preparation
60 and measurement routines. This included extensive work on instrumental isotopic fractionation
61 corrections, ICP operating conditions or the identification, elimination and control of spectral
62 interferences and blanks (Archer and Vance, 2004; Bermin et al., 2006; Petit et al., 2008). Early
63 studies used an in-house Zn ICP standard purchased from Johnson and Matthey (so called JMC
64 Lyon standard) as 0-anchor (Maréchal et al., 1999). Since this standard is now exhausted, the
65 Commission on Isotopic Abundances and Atomic Weights (CIAAW) suggests the IRMM-
66 3702 (Ponzevera et al., 2006) to be used as new 0-anchor (Brand et al., 2014). A re-evaluation
67 of this material by Moeller et al. (2012) resulted in a $\delta^{66}\text{Zn}/^{64}\text{Zn}_{\text{IRMM-3702}}$ value of -0.29 ‰ for
68 the JMC standard. Up to now, the IRMM-3702 is the only standard with published absolute
69 isotope-amount ratios, commercially available and fulfilling all criteria to be used as 0-anchor
70 on an isotope-delta scale as used by CIAAW. The second available isotope standard is the AA-
71 ETH Zn that is so far believed to be isotopically indistinguishable from the IRMM-3702
72 (Archer et al., 2017).

73 Zn is a ubiquitous trace metal with an essential role as micronutrient. Furthermore, Zn is widely
74 used in industrial processes for e.g. electroplating, for alloy production and as anti-corrosion
75 coating. With a worldwide production of 11.9 million metric tons (in 2016), Zn is one of the
76 most important metals and therefore a critical source of anthropogenic contamination (Survey,
77 2017). John et al. (2007b) who investigated the isotopic composition of common forms of
78 anthropogenic Zn, suggested to make use of Zn isotope signatures as potential environmental
79 tracer. Significant isotopic fractionation of Zn metal-based products, which causes the
80 depletion of heavy isotopes in blast furnace emissions ($\delta^{66}\text{Zn}/^{64}\text{Zn}_{\text{JMC-Lyon}} = -0.36 \text{ ‰}$) (Mattielli
81 et al., 2009) and enrichment in heavy isotopes in effluents ($\delta^{66}\text{Zn}/^{64}\text{Zn}_{\text{JMC-Lyon}} = 0.41 \text{ ‰}$)
82 (Arnold et al., 2010) and slags ($\delta^{66}\text{Zn}/^{64}\text{Zn}_{\text{JMC-Lyon}} = 0.18 \text{ ‰}$ to 1.49 ‰) (Sivry et al., 2008) has
83 been described. Other high-temperature processes like coal combustion are also known to
84 induce significant isotopic fractionation leading to the enrichment of heavy Zn isotopes in e.g.
85 fly ash, while flue gases are enriched in lighter Zn isotopes (Gonzalez and Weiss, 2015).
86 Even though the use of Zn isotopic signatures as a tracer of anthropogenic emissions has been
87 demonstrated and highlighted in various studies, examples on their application to samples from
88 river and coastal environments are still scarce today (Gonzalez et al., 2016; Thapalia et al.,
89 2015). The first studies were published by Petit et al. (2008) who analyzed suspended
90 particulate matter and sediments from the Scheldt estuary, revealing significant differences in
91 isotopic composition of $\delta^{66}\text{Zn}/^{64}\text{Zn}_{\text{JMC-Lyon}}$ between 0.22 ‰ and 1.13 ‰ for surface sediment
92 samples. Studies by Sivry et al. (2008) and Araújo et al. (2017) focused on relatively small
93 sampling areas (Sivry et al., ca. $10 \times 10 \text{ km}$; Araújo et al. ca. $15 \times 30 \text{ km}$) with well-known
94 anthropogenic emission by Zn ore treatment plants. In both studies $\delta^{66}\text{Zn}/^{64}\text{Zn}_{\text{JMC-Lyon}}$ values
95 for sediment samples of up to 1.35 ‰ have been found, which is significantly higher than the
96 corresponding geogenic background. Work by Chen et al. (2008; 2009) are the only studies
97 providing $\delta^{66}\text{Zn}/^{64}\text{Zn}$ data obtained from a large anthropogenically impacted sampling area, so

98 far. Their investigation of the Seine River in France showed significant isotopic variations in
99 water samples with $\delta^{66}\text{Zn}/^{64}\text{Zn}_{\text{JMC-Lyon}}$ ranging from 0.07 ‰ to 0.58 ‰ and a $\delta^{66}\text{Zn}/^{64}\text{Zn}_{\text{JMC-Lyon}}$
100 ranging from 0.08 ‰ to 0.30 ‰ for suspended matter, with a distinctly lighter isotopic
101 composition in downstream areas of the Seine. The city of Paris was found to cause a
102 significant input of anthropogenic Zn originating from roadway and roof runoff, resulting in a
103 generally lighter isotopic composition ($\delta^{66}\text{Zn}/^{64}\text{Zn}_{\text{JMC-Lyon}} = -0.11 \text{ ‰ to } 0.02 \text{ ‰}$) of the
104 investigated samples.

105 This study focused on the analysis of the Zn isotopic variation in water and surface sediment
106 samples from one of largest European rivers, the Elbe. With its catchment area of 148 000 km²
107 the Elbe River is the fourth largest river in Central Europe (Bohlich and Strotmann, 2008). For
108 decades, it was considered as one of the most contaminated rivers in Europe. The Elbe and its
109 pollution load have been subject to researchers from several disciplines (Brase et al., 2017;
110 Prange et al., 2001; Prange et al., 1997; Sühling et al., 2015). Since the work of Prange et al.
111 that was conducted in the 1990s, only a limited number of further studies focused on the topic
112 of metal contamination. Only recently, the first work on the use of non-traditional stable isotope
113 ratios as tracers for environmental processes in the study area of the Elbe River was published
114 by Reese et al. (2019). The authors reported stable isotope ratios of Sr, Nd and Pb beside multi-
115 element data of surface sediments from the Elbe estuary. Results clearly proved the potential
116 of “non-traditional” isotope ratio analysis as a valuable tool to describe areas under both,
117 natural and anthropogenic influence. Reese et al. (2019) focused on the interpretation of metal
118 contamination within the context of environmental research related to complex land-river-sea
119 systems.

120 In this study, we extend the palette of non-traditional stable isotopes used as tracers in the Elbe
121 catchment with stable Zn isotope ratios, in order to further explore the usage of isotopic tools
122 in aquatic ecosystem studies. The main objective of our work was to investigate the variation

123 of natural Zn isotopic composition in water and sediment in a river ecosystem at large scale
124 and evaluate the applicability of Zn isotope ratios as tracer for anthropogenic Zn emissions.
125 Furthermore, this work addressed possible processes that potentially cause natural isotopic
126 fractionation within the river and its catchment.

127 **2. Experimental**

128 **2.1 Materials, reagents and reference materials**

129 The marine sediment GBW-07313 (National Research Centre for Certified Reference
130 Materials, Beijing, China) and the basalt BCR-2 (U.S. Geological Survey, Reston, USA) were
131 used as reference materials for Zn quantification in sediment digests and the riverine waters
132 SLRS-1 and SLRS-3 (National Research Council of Canada, Ottawa, Canada) were used as
133 reference materials for Zn quantification in water samples. Custom-made multi-elemental
134 standards (Inorganic Ventures, Christiansburg, USA) were used for preparation of external
135 calibrations for quantification via ICP-MS. The isotopic reference material IRMM-3702 (Joint
136 Research Centre, Geel, Belgium) was used for calibration of the double spike.

137 Experimental work was carried out at the Helmholtz-Zentrum Geesthacht and at the University
138 of Calgary. Preparatory laboratory work carried out at the Helmholtz-Zentrum Geesthacht
139 included sieving and digestion of the sediment samples, filtration of the water samples, multi-
140 element quantification measurements and evaporation of the samples to dryness prior to sample
141 preparation for Zn isotopic analysis. The evaporated samples were shipped to the University of
142 Calgary, where column separation and isotopic analysis of Zn were accomplished. Method
143 blanks were processed to monitor the entire procedure including shipping.

144

145 *Helmholtz-Zentrum Geesthacht, Germany*

146 All sample preparation steps carried out at Department of Marine Bioanalytical Chemistry,
147 Institute of Coastal Research, were performed in a class 10000 clean room inside a class 100
148 clean bench to minimize blank levels and any risks of contamination. Suprapur[®] nitric acid
149 (65% w/w, Merck-Millipore, Darmstadt, Germany) and suprapur[®] hydrochloric acid (30% w/w,
150 Merck-Millipore, Darmstadt, Germany) were further purified by double sub-boiling in quartz
151 stills (AHF Analysentechnik, Tübingen, Germany). Tetrafluoroboric acid (38% w/w) used for
152 sample digestion was purchased from Chem-Lab (Zedelgem, Belgium) and used without any
153 further purification. Ultra-pure water (18.2 MΩ*cm) used for analysis and cleaning was
154 obtained from a Milli-Q ElementQ/QPod Element water purification system (Merck-Millipore,
155 Darmstadt, Germany).

156

157 *University of Calgary, Canada*

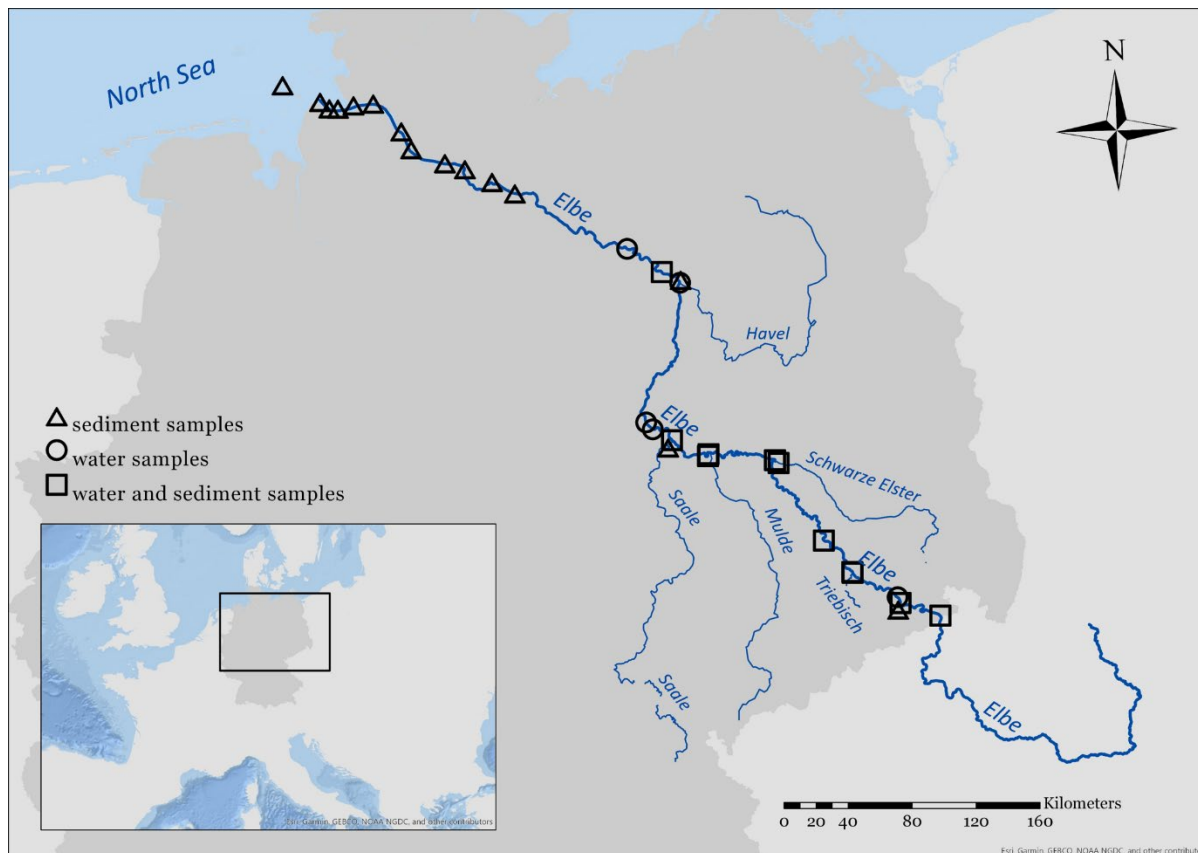
158 All sample preparation steps carried out at the Department of Physics and Astronomy were
159 performed in a class 1000 clean room inside a clean bench to minimize blank levels and any
160 risks of contamination. Aristar[®] Ultra nitric acid (65% w/w, VWR International, Radnor, USA)
161 and environmental grad plus hydrochloric acid (32-35% w/w, VWR International, Radnor,
162 USA) were used. Ultra-pure water used for analysis and cleaning was obtained from a water
163 purification system with a resistivity of 18.2 MΩ*cm. Enriched ⁶⁴Zn and ⁶⁷Zn materials used
164 for the preparation of the double spike were purchased in oxide form from Oak Ridge National
165 Laboratory (Oak Ridge, USA). The zinc double spike $n(^{66}\text{Zn})/n(^{67}\text{Zn})$ isotope-amount ratio was
166 ~4.88 in order to achieve the most precise isotope-amount ratios as recommended by Rudge et
167 al. (2009).

168 **2.2 Samples and sample preparation**

169 Surface sediment and water samples from the river Elbe were obtained in the course of a
170 sampling campaign conducted in August and September 2015 between the Elbe estuary

171 (German Elbe river kilometer 757) and the German Czech border (German Elbe river kilometer
172 0). The sampling area is shown in Fig. 1. In total 26 sediment and 17 water samples were
173 analyzed in this study.

174



175

176 **Fig. 1.** Map of the Elbe River from the German Czech boarder (river km 0) to the mouth into
177 the North Sea (river km 757). The sampling locations at which sediment samples were taken
178 are marked as triangle, water sampling locations as circle and locations were both, water and
179 sediment samples, were taken are marked as square.

180

181 2.2.1 Sampling locations

182 The part of the Elbe River impacted by the tide starts at river kilometer 757 up to the weir
183 Geesthacht at river kilometer 587. Therefore, within the estuary, the sampling locations S_01
184 Scharnhörnriff to S_11 Geesthacht were selected. Hamburg is the largest city within the estuary
185 with the third largest port in Europe. Samples upstream of river kilometer 588 up to the

186 German/Czech boarder at river kilometer 0 were taken between Lauenburg (sample S_12
187 Lauenburg) and Schmilka (sample S_31 Schmilka). Within this river section, sampling also
188 included locations in the main tributaries, the Havel (S_16 Tb. Havel), the Saale (S_20 Tb.
189 Saale) and the Mulde (S_22 Tb. Mulde), as well as some smaller tributaries, the Schwarze
190 Elster (S_24 Tb. Schwarze Elster), the Triebisch (S_27 Tb. Triebisch) and the Müglitz (S_30
191 Tb. Müglitz). All sampling locations in tributaries are labeled Tb. A detailed description of
192 sampling coordinates including river kilometers can be found in the Supplemental information
193 Table A1.

194 Sampling locations in this study were selected based on the original locations reported in the
195 1990s by Prange et al. to allow for direct comparison of data in a time-dependent perspective.
196 However, the impact of tributaries to the Elbe River were considered in the study by Prange et
197 al. by taking samples at the tributary's mouth into the Elbe River only. In this study tributaries
198 were sampled not only at the tributary's mouth but also several kilometers upstream the
199 respective tributary before it discharges into the Elbe River.

200 **2.2.2 Sediment samples**

201 A detailed description of the sediment sample preparation and digestion process, including
202 recoveries of elemental mass fractions of the marine sediment reference material GBW-07313
203 and the basalt reference material BCR-2 can be found elsewhere (Reese et al., 2019). Both
204 reference materials were quantitatively digested using the presented digestion method resulting
205 in clear, particle free digests. Surface sediment samples were collected by using a custom-made
206 box corer. The top layer (5 to 10 cm) of three or more individual samplings were subsequently
207 homogenized, deep-frozen, freeze dried (Martin Christ Gefriertrocknungsanlagen, Osterode,
208 Germany) and sieved over a cascade of polyamide sieves (Atechnik, Leinburg, Germany) to
209 obtain the <63 μm fraction. About 50 mg of the sieved sediment material was weighed into 55
210 mL TFM® bombs and 5 mL concentrated double sub-boiled nitric acid, 2 mL concentrated

211 double sub-boiled hydrochloric acid and 1 mL tetrafluoroboric acid were added. The samples
212 were digested for 300 minutes at 180 °C using a MARS 5 Xpress (CEM Corp., Kamp Lintfort,
213 Germany) microwave. Digestion of each sample was carried out in triplicates, quantitatively
214 transferred to 50 mL pre-cleaned DigiTUBEs (SCP Science, Quebec, Canada) and diluted to a
215 final volume of 50 mL with Milli-Q water. Based on the measured Zn mass fraction an amount
216 equivalent to 500 ng Zn was transferred from one of the three digests to a 50 mL pre-cleaned
217 DigiTUBE, evaporated to dryness, sealed and shipped to the University of Calgary. This
218 required the evaporation of up to 15 mL of sample depending on the initial Zn mass fraction.

219 **2.2.3 Water samples**

220 The pH-value of the water samples was measured in an aliquot of the sample before filtration
221 using a portable pH probe (Multi 3430, WTW, Germany). Water samples were filtered in
222 triplicates using a custom built pressure filtration system made of high purity PFA filtration
223 bombs (Savillex, Eden Prairie, USA) and acid washed 0.4 µm polycarbonate filters (Whatman,
224 Maidstone, United Kingdom). The bombs were pressurized with high purity nitrogen or argon.
225 After filtration, the samples were acidified with 500 µL concentrated double sub-boiled nitric
226 acid and stored in 500 mL LDPE Nalgene® bottles (Thermo Fisher Scientific, Schwerte,
227 Germany) at 4 °C. Based on the measured Zn concentration in the individual sample, a sample
228 volume containing an equivalent to 500 ng Zn in total from one sample of each sampling
229 location was transferred to a 50 mL pre-cleaned DigiTUBE, evaporated to dryness and shipped
230 to the University of Calgary. This required the evaporation of up to 150 mL of sample.

231 **2.2.4 Ion extraction of Zn**

232 Prior to ion extraction the evaporated samples were doped with 500 ng of Zn double spike,
233 equilibrated, evaporated again to dryness in a DigiPrep evaporation system under a HEPA-
234 filtered hood (SCP Science, Quebec, Canada) and re-dissolved in 1.5 mL of 1 mol L⁻¹

235 hydrochloric acid in an ultrasonic bath. Isolation of Zn was accomplished by using the anion
236 exchange resin AG MP-1 (100-200 mesh size, Bio-Rad, Hercules, USA) according to a
237 modified separation scheme published by Moore et al. (2017). Prior to usage, the suspended
238 resin (in 0.5 mol L⁻¹ hydrochloric acid) was cleaned with 0.5 mol L⁻¹ nitric acid and water.
239 Approximately 250 µL of the resin were packed into leached custom made glass micro
240 columns. After the first ion-extraction cycle, samples with high Ba content were further
241 purified by using Sr Resin (TrisKem International, Bruz, France) in order to remove residual
242 Ba, which could potentially interfere as Ba²⁺ on ⁶⁶Zn, ⁶⁷Zn and ⁶⁸Zn. A detailed description of
243 the ion extraction protocols for both separation cycles can be found in the Supplemental
244 information Table A2.

245

246 **2.3 Instrumentation and measurement procedures**

247 **2.3.1 Elemental analysis**

248 The determination of Zn mass fractions in the sediment digests and Zn concentrations in filtered
249 water samples was performed using an inductively coupled plasma tandem mass spectrometer
250 (ICP-MS/MS) (Agilent 8800, Agilent Technologies, Tokyo, Japan) coupled to an ESI SC-4
251 DX FAST autosampler (Elemental Scientific, Omaha, Nebraska, USA) at the Helmholtz-
252 Zentrum Geesthacht. For quantification an external calibration, prepared from custom-made
253 multi-elemental standards ranging from 0.1 µg L⁻¹ to 100 µg L⁻¹ was used. Solutions were
254 prepared on a daily basis. A detailed description of the instrument configuration can be found
255 in the Supplemental information Table A3.

256 Multi-elemental data were processed using MassHunter version 4.2 and a custom-written
257 Excel[®] spreadsheet. Recoveries were calculated using the marine reference sediment GBW-
258 07313 and riverine reference waters SLRS-1 and SLRS-3. Combined uncertainties were

259 calculated using a simplified Kragten (1994) approach taking into account reproducibility,
260 repeatability and measurement precision for amount fractions in sediment samples and
261 reproducibility and measurement precision for concentrations in water samples. Samples were
262 analyzed as triplicates, using three individual digests/filtrates. Recoveries for the used reference
263 materials GBW-07313, SLRS-1 and SLRS-3 are shown in the Supplemental information Table
264 A4.

265

266 **2.3.2 Isotopic analysis**

267

268 Zn isotope-amount ratios were measured at the University of Calgary using a Neptune MC
269 ICP-MS (Thermo Fisher Scientific, Bremen, Germany) operated in low mass resolution mode.
270 A 20-mL cyclonic spray chamber (Glass Expansion, Pocasset, USA) fitted with a glass
271 nebulizer (sample uptake of $100 \mu\text{L min}^{-1}$) was used as sample introduction system. A detailed
272 description of the instrument configuration can be found in the Supplemental information Table
273 A3.

274 Faraday cups H2, C, L1, L2, L4 were used to measure the ion beams of ^{64}Zn , ^{66}Zn , ^{67}Zn , ^{68}Zn
275 and ^{70}Zn . Sample measurements consisted of one block with 30 measurements. In order to
276 correct for potential Ni interferences occurring on ^{64}Zn , one measurement of 8 s integration
277 time prior to the measurement of Zn was used. During this 8 s measurement, ^{60}Ni was
278 monitored on faraday cup C, ^{62}Ni on L2 and ^{64}Zn on L4, respectively. Due to adjusted zoom
279 optic voltages, no magnet jump was needed.

280 Typical sensitivities were around 8 V for $1 \mu\text{g mL}^{-1}$ ^{64}Zn with blank values of 2 mV.
281 Instrumental isotopic fractionation correction was achieved with a $^{64}\text{Zn}+^{67}\text{Zn}$ double spike,
282 which was calibrated against the certified material IRMM-3702. Sample and standards were

283 doped with equal amounts of double spike (1:1 ratio) leading to a final Zn concentration of 500
284 ng mL⁻¹ for each sample.

285 Zn isotopic compositions are reported as $\delta^{66}\text{Zn}/^{64}\text{Zn}_{\text{IRMM-3702}}$ expressed as parts per thousand
286 (‰) relative to the Zn IRMM standard IRMM-3702 calculated by Eq. 1.

287

$$288 \quad \delta^{66}\text{Zn}/^{64}\text{Zn}_{\text{IRMM-3702}} = \left(\frac{{}^{66}\text{Zn}/{}^{64}\text{Zn}_{\text{Sample}}}{{}^{66}\text{Zn}/{}^{64}\text{Zn}_{\text{IRMM-3702}}} - 1 \right) \quad (1)$$

289

290 We refer to $\delta^{66}\text{Zn}/^{64}\text{Zn}_{\text{IRMM-3702}}$ throughout the manuscript. A conversion to $\delta^{66}\text{Zn}/^{64}\text{Zn}_{\text{JMC-Lyon}}$
291 is available in the Supplemental Information.

292 Data processing of the raw ratios was done offline using a data reduction program written by
293 Alex Tennant (University of Calgary) in Python™. The program employs root finding
294 algorithms to solve the double spike equations as described by Rudge et al. (2009). The code
295 includes blank correction and correction for instrumental isotopic fractionation based on the
296 $^{64}\text{Zn}/^{67}\text{Zn}$ isotope-amount ratio of the double spike. The double spike was calibrated against
297 IRMM-3702 via internal isotopic fractionation correction using a $^{66}\text{Zn}/^{68}\text{Zn}$ ratio for IRMM-
298 3702 of 0.66525 (Moeller et al., 2012). The spectral interference of ^{64}Ni on mass ^{64}Zn was
299 found to be negligible and was therefore not corrected. For quality control, IRMM-3702 spiked
300 with the double spike as well as IRMM-3702 following ion extraction were run routinely,
301 multiple times every day. For isotope data combined uncertainties were calculated taking into
302 account measurement precision and reproducibility of the used IRMM-3702 standard. (Note:
303 The 0-anchor material is not assigned with an uncertainty per definition.)

304 **3 Results**

305 **3.1 Validation and performance characteristics of the analytical method**

306 The suitability of the modified sample preparation protocol for water and sediment samples
307 was evaluated with respect to different analytical parameters. Recoveries for the IRMM-3702
308 reference material after ion extraction yielded values of $108\% \pm 7\%$ ($n=4$), indicating a
309 quantitative recovery of Zn. Furthermore, measured recoveries of the separated water and
310 sediment samples ranged from 88% to 113% (with a mean of $98\% \pm 6\%$, $n=44$) based on the
311 measured standard to double spike ratio. Procedural Zn blanks for the ion extraction protocol
312 were $1.0 \text{ ng} \pm 0.2 \text{ ng}$ ($n=6$), which was negligible for a total sample amount of 500 ng Zn.
313 Measurements of the IRMM-3702 reference material yielded an external between-run
314 precision of $\delta^{66}\text{Zn}/^{64}\text{Zn}_{\text{IRMM-3702}} = -0.02 \text{ ‰} \pm 0.10 \text{ ‰}$ ($U(k=1)$, $n=22$) for a total of 5
315 measurement days.

316 **3.2 Concentration measurements and isotopic data**

317 All sampling locations, including measured Zn concentrations/mass fractions and Zn isotopic
318 compositions ($\delta^{66}\text{Zn}/^{64}\text{Zn}_{\text{IRMM-3702}}$) can be found in the Supplemental information Table A1.
319 Note: Historical samples by Prange et al. had been taken at the same sampling coordinates. Zn
320 mass fractions for historical sediment samples were measured in $<20 \text{ }\mu\text{m}$ grain size fractions,
321 water samples were filtered via $0.45 \text{ }\mu\text{m}$ filters, respectively.

322 **3.3.1 Zn mass fractions and $\delta^{66}\text{Zn}/^{64}\text{Zn}_{\text{IRMM-3702}}$ in sediment samples**

323 Zn mass fractions for sediment samples ranged from 42 mg kg^{-1} to 1120 mg kg^{-1} along the
324 course of the Elbe (see Table A1 and Fig. 2A). The average mass fraction of all sediment
325 samples analyzed in this study was $417 \text{ mg kg}^{-1} \pm 294 \text{ mg kg}^{-1}$ (1 SD, $n=26$). The lowest
326 measured mass fraction of around 42 mg kg^{-1} was found in the estuary (S_01 Scharhörnriff, km

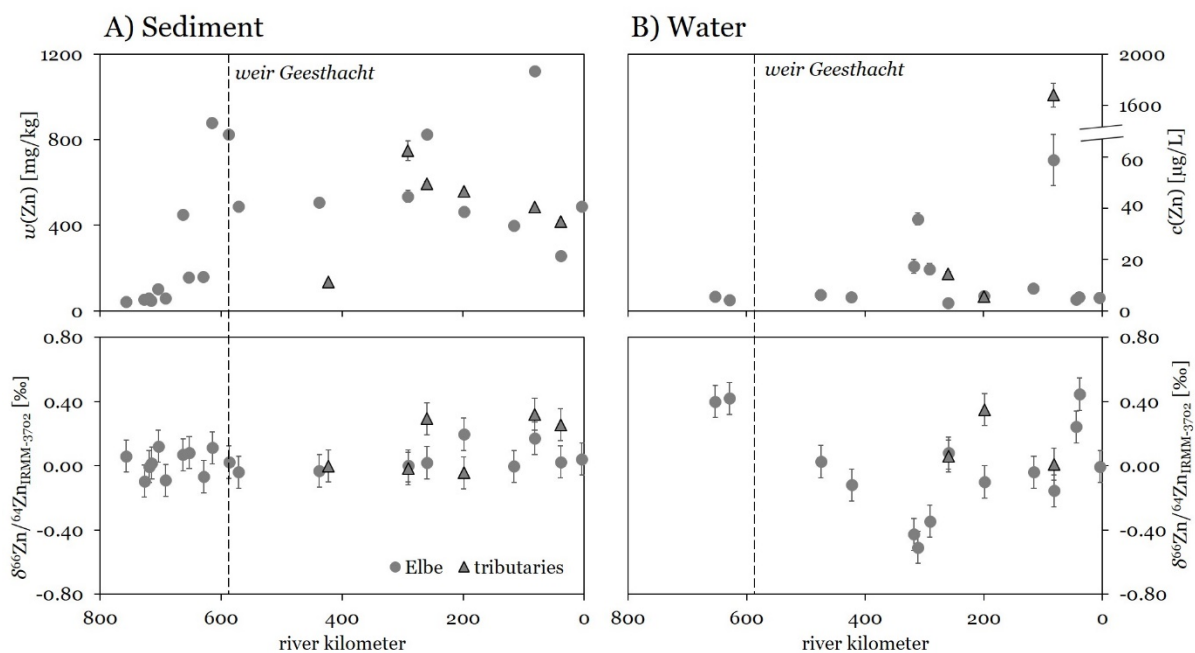
327 757). Elevated mass fractions of 879 mg kg⁻¹ and 826 mg kg⁻¹ were measured for two sampling
328 locations upstream the city of Hamburg (S_10 Billwerder Inseln, km 615 and S_11 Geesthacht,
329 km 587). Mass fractions upstream the weir in Geesthacht were highly variable ranging from
330 135 mg kg⁻¹ for the Havel River (S_16 Tb. Havel, km 423) to 1120 mg kg⁻¹ measured in the
331 Elbe River near the mouth of the tributary Triebisch (S_26 Triebisch, km 82). Elevated Zn
332 mass fractions could also be found in two major tributaries of the Elbe River, the Saale (750
333 mg kg⁻¹, S_20 Tb. Saale, km 291) and the Mulde (593 mg kg⁻¹, S_22 Tb. Mulde, km 260).
334 Zn isotopic compositions expressed as $\delta^{66}\text{Zn}/^{64}\text{Zn}_{\text{IRMM-3702}}$ of sediment samples ranged from -
335 0.10 ‰ to 0.32 ‰. Taking into account the analytical uncertainty of 0.10 ‰ ($U(k=1)$) most of
336 the samples were not significantly different from each other. In addition, three sampling
337 locations with significantly heavier isotopic compositions could be identified. All of them are
338 assigned to tributaries of the Elbe River, namely the Mulde ($\delta^{66}\text{Zn}/^{64}\text{Zn}_{\text{IRMM-3702}}$ 0.29 ‰ \pm 0.10
339 ‰, S_22 Tb. Mulde, km 260), the Triebisch ($\delta^{66}\text{Zn}/^{64}\text{Zn}_{\text{IRMM-3702}}$ 0.32 ‰ \pm 0.10 ‰, S_27 Tb.
340 Triebisch, km 82) and the Müglitz ($\delta^{66}\text{Zn}/^{64}\text{Zn}_{\text{IRMM-3702}}$ 0.26 ‰ \pm 0.10 ‰, S_30 Tb. Müglitz,
341 km 39).

342 **3.3.2 Zn concentrations and $\delta^{66}\text{Zn}/^{64}\text{Zn}_{\text{IRMM-3702}}$ in water samples**

343 Dissolved Zn concentrations for water samples ranged from 3.2 $\mu\text{g L}^{-1}$ to 1680 $\mu\text{g L}^{-1}$. The
344 average concentration of all water samples of this study (except sample S_27 Tb. Triebisch)
345 was 12.6 $\mu\text{g L}^{-1} \pm 14.4 \mu\text{g L}^{-1}$ (1 SD, $n=16$). Most measured Zn concentrations were found to
346 be lower than 10 $\mu\text{g L}^{-1}$ with only a few exceptions (see Table A1 and Fig. 2B). Concentrations
347 higher than 10 $\mu\text{g L}^{-1}$ were observed for the two sampling locations S_17 Magdeburg at km
348 318 (17.3 $\mu\text{g L}^{-1}$) and S_18 Schönebeck at km 311 (35.8 $\mu\text{g L}^{-1}$) within the Elbe. Significantly
349 elevated concentrations were also found for sampling locations deducted to tributaries, namely
350 the mouth of the Saale (16.4 $\mu\text{g L}^{-1}$, S_19 Saale, km 291), the tributary Mulde (14.4 $\mu\text{g L}^{-1}$,
351 S_22 Tb. Mulde, km 260) and the mouth of the tributary Triebisch (58.7 $\mu\text{g L}^{-1}$, S_26 Triebisch,

352 km 82). An extremely elevated concentration of dissolved Zn of 1680 $\mu\text{g L}^{-1}$ was observed for
 353 the tributary Triebisch (S_27 Tb. Triebisch, km 82).
 354 The Zn isotopic composition of water samples showed higher relative variability compared to
 355 the sediment samples with $\delta^{66}\text{Zn}/^{64}\text{Zn}_{\text{IRMM-3702}}$ ranging from -0.51 ‰ to 0.45 ‰. For samples
 356 taken in the estuary (S_08 Tonne 107, km 653 and S_09 Seemannshöft, km 629) generally
 357 higher $\delta^{66}\text{Zn}/^{64}\text{Zn}_{\text{IRMM-3702}}$ values than those for the riverine samples upstream were observed
 358 ($\delta^{66}\text{Zn}/^{64}\text{Zn}_{\text{IRMM-3702}}$ 0.40 ‰ \pm 0.10 ‰, $\delta^{66}\text{Zn}/^{64}\text{Zn}_{\text{IRMM-3702}}$ 0.43 ‰ \pm 0.10 ‰). A comparable
 359 high $\delta^{66}\text{Zn}/^{64}\text{Zn}_{\text{IRMM-3702}}$ value was also observed for the tributary Schwarze Elster
 360 ($\delta^{66}\text{Zn}/^{64}\text{Zn}_{\text{IRMM-3702}}$ 0.35 ‰ \pm 0.10 ‰, S_24 Tb. Schwarze Elster, km 199). Additionally, a
 361 $\delta^{66}\text{Zn}/^{64}\text{Zn}_{\text{IRMM-3702}}$ value of 0.45 ‰ \pm 0.10 ‰ was observed in the Elbe River near the mouth
 362 of the tributary Müglitz (S_29 Müglitz, km 39). In contrast to this, significantly lower
 363 $\delta^{66}\text{Zn}/^{64}\text{Zn}_{\text{IRMM-3702}}$ values of -0.43 ‰ \pm 0.10 ‰, -0.51 ‰ \pm 0.10 ‰ and -0.34 ‰ \pm 0.10 ‰
 364 were observed for the three sampling locations S_17 Magdeburg, S_18 Schönebeck and S_19
 365 Saale (km 291-318), respectively.

366
 367



368
 369 **Fig. 2.** A) Zn mass fractions and $\delta^{66}\text{Zn}/^{64}\text{Zn}_{\text{IRMM-3702}}$ values for collected sediment samples in
 370 the course of the Elbe River and its tributaries. B) Zn concentrations and $\delta^{66}\text{Zn}/^{64}\text{Zn}_{\text{IRMM-3702}}$

371 values for collected water samples in the course of the Elbe River and its tributaries. Sampling
372 locations are sorted according to the German Elbe river kilometer. (Error bars correspond to U
373 ($k = 1$) for isotopic data and to U ($k = 2$) for mass fractions and concentrations, respectively (if
374 not visible $U =$ smaller than spotsize)
375

376 **4 Discussion**

377 **4.1 Comparison with historical data published by Prange et al.**

378 When comparing Zn mass fractions in sediment samples from this study to historical data, it
379 has to be noted that Zn mass fractions were measured in different grain size fractions (this study
380 $<63 \mu\text{m}$, Prange et al. $<20 \mu\text{m}$). Since heavy metal mass fractions in different grain size
381 fractions can significantly vary, a direct comparison to historical sediment data is challenging
382 (Ackermann et al., 1983). Nevertheless, the historical data can give valuable information about
383 the origin of concentration hotspots within the Elbe River. In contrast to that, concentration
384 data of dissolved Zn in the water phase is directly comparable between both datasets.

385

386 **4.1.1 Comparison of Zn mass fractions in sediment samples to historical data**

387 Prange et al. published median Zn mass fractions in Elbe sediments for all analyzed samples
388 from the confluence of Mulde and Elbe to the estuary (river kilometer 650 – 260) of 2530 mg kg^{-1}
389 kg^{-1} (1992) and 1820 mg kg^{-1} (1995). Historical Zn mass fractions of sampling locations S_19
390 Saale (3026 mg kg^{-1} (1992), 2452 mg kg^{-1} (1995)), S_21 Mulde (3379 mg kg^{-1} (1992), 4887 mg
391 kg^{-1} (1995)) and S_26 Triebisch (23800 mg kg^{-1} (1992), 8442 mg kg^{-1} (1995)), indicate that the
392 corresponding tributaries carried high loads of Zn at the time. Additionally, published Zn
393 median mass fractions decreased during the study period from 2530 mg kg^{-1} in 1992 to 1420
394 mg kg^{-1} in 1998, indicating a decrease of Zn emissions into the Elbe River.

395 The average Zn mass fractions in sediment samples of this study was 417 mg kg^{-1} , which is
396 significantly lower than historical data. In comparison with recent data from other European
397 river systems e.g. the Danube average Zn mass fractions were significantly lower than in the
398 Elbe River ($187 \text{ mg kg}^{-1} \pm 25 \text{ mg kg}^{-1}$ in $<63 \mu\text{m}$ grain size fraction) (Woitke et al., 2003).
399 Estimated geogenic background concentrations for the Elbe River range between 50 mg kg^{-1}
400 and 200 mg kg^{-1} (only available for $<20 \mu\text{m}$ fraction) (LAWA, 1998). (For some sampling
401 locations, such as S_21 Mulde at km 260 (824 mg kg^{-1} (this study)) and S_26 Triebisch at km
402 82 (1120 mg kg^{-1} (this study)) Zn mass fractions in the sediment samples are still higher than
403 the average load of the Elbe River. This might still make these tributaries potential sources of
404 anthropogenic Zn emissions into the Elbe River e.g. originating from old mining activities.

405 **4.1.2 Comparison of Zn concentrations in water samples to historical data**

406 The average discharge volume of the Elbe River increases from $315 \text{ m}^3 \text{ s}^{-1}$ at the German/Czech
407 boarder to $877 \text{ m}^3 \text{ s}^{-1}$ at the mouth of the estuary. The most important tributaries are the Havel
408 $115 \text{ m}^3 \text{ s}^{-1}$, the Saale $115 \text{ m}^3 \text{ s}^{-1}$, the Mulde $73 \text{ m}^3 \text{ s}^{-1}$ and the Schwarze Elster $28 \text{ m}^3 \text{ s}^{-1}$ (ATV-
409 DVWK, 2000). During August/September 2015 the average discharge of the Elbe River was
410 approximately $240 \text{ m}^3 \text{ s}^{-1}$ that is considered as a dry period with low water discharge (IKSE,
411 2017). For water samples taken in September 1995 and 1998 by Prange et al. the discharge
412 volumes were approximately $990 \text{ m}^3 \text{ s}^{-1}$ and $320 \text{ m}^3 \text{ s}^{-1}$, respectively. Historical median
413 concentrations of the dissolved Zn fraction in Elbe water samples between river kilometer 650
414 and 260 varied between $16.5 \mu\text{g L}^{-1}$ (1992) and $3.0 \mu\text{g L}^{-1}$ (1995) respectively. An estimated
415 geogenic background of dissolved Zn in unpolluted German Rivers lies in the range of $1 \mu\text{g L}^{-1}$
416 (LAWA, 1998).

417 Historical data showed significantly higher Zn concentrations for some sampling locations at
418 the confluence of tributaries. This included samples taken at the locations S_19 Saale ($50.5 \mu\text{g}$
419 L^{-1} (1995), $55.8 \mu\text{g L}^{-1}$ (1998)), S_21 Mulde ($109.9 \mu\text{g L}^{-1}$ (1995), $3.95 \mu\text{g L}^{-1}$ (1998)), S_23

420 Schwarze Elster (47.5 $\mu\text{g L}^{-1}$ (1995), 5.37 $\mu\text{g L}^{-1}$ (1998)), S_26 Triebisch (1490 $\mu\text{g L}^{-1}$ (1995),
421 1780 $\mu\text{g L}^{-1}$ (1998)) and S_29 Müglitz (32.1 $\mu\text{g L}^{-1}$ (1995), 15.8 $\mu\text{g L}^{-1}$ (1998)). For some of
422 these sampling locations, a decrease of Zn concentrations could be observed over time (S_21
423 Mulde, S_23 Schwarze Elster), whereas at some sampling locations the measured Zn
424 concentrations remained constant (S_19 Saale, S_26 Triebisch). Our data indicated that even
425 today some tributaries carry significantly higher dissolved Zn amounts than the Elbe River
426 itself, namely the Mulde (14.4 $\mu\text{g L}^{-1}$, S_22 Tb. Mulde, km 260) and the Triebisch (1680.0 μg
427 L^{-1} , S_27 Tb. Triebisch, km 82) making tributaries a potential source of anthropogenic Zn
428 contamination. Especially, the tributary Triebisch that still contains high amounts of dissolved
429 Zn.

430 In summary, Zn concentrations in sediment and water clearly decreased during the last three
431 decades indicating a substantial decrease of anthropogenic Zn emissions into the Elbe River,
432 an observation also described by other authors (Vink et al., 1999). Nevertheless, some sampling
433 locations are still characterized by elevated Zn concentrations.

434

435 **4.2 Zn isotopic signatures of sediment samples**

436 A detailed description of the underlying geology is shown in Fig. 3. Most of the catchment area
437 is characterized by glacial deposits. Nevertheless, the surface geology significantly changes
438 upstream and tributaries originating in the Ore Mountains (e.g. Mulde, Triebisch und Müglitz)
439 feature a significant change in surface geology of their catchments. The catchment area of these
440 tributaries is mainly characterized by metamorphic and igneous bedrock (Rohstoffe, 2006).

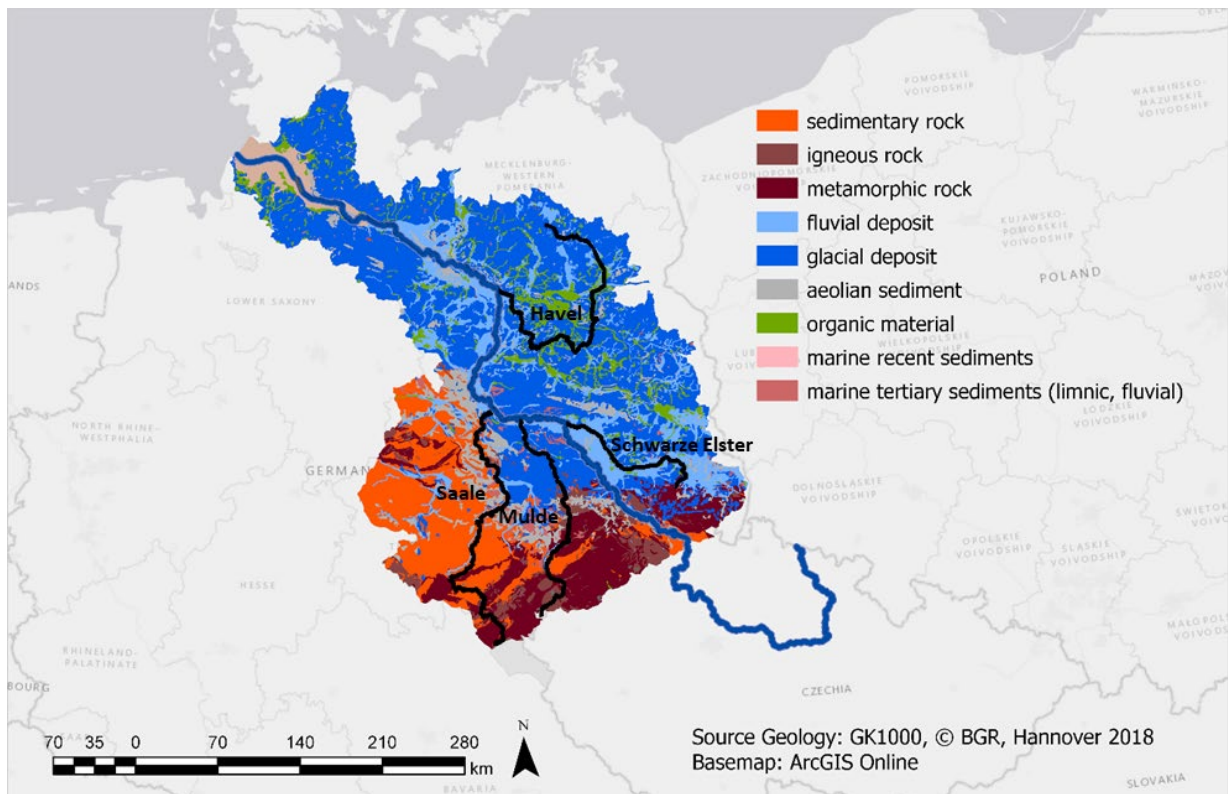
441 Our study revealed no significant changes in isotopic composition of $\delta^{66}\text{Zn}/^{64}\text{Zn}_{\text{IRMM-3702}}$ for
442 sediment samples taken in the Elbe River with a mean of $0.05\text{‰} \pm 0.11\text{‰}$. In fact, measured
443 $\delta^{66}\text{Zn}/^{64}\text{Zn}_{\text{IRMM-3702}}$ are in accordance to the terrestrial background of $\delta^{66}\text{Zn}/^{64}\text{Zn}_{\text{IRMM-3702}} -0.01$
444 $\text{‰} \pm 0.05\text{‰}$ (corresponding to $\delta^{66}\text{Zn}/^{64}\text{Zn}_{\text{JMC-Lyon}}$ of $0.28\text{‰} \pm 0.05\text{‰}$) as published by Chen

445 et al. (2013). Regarding the Elbe River estuary, a thorough mixing of sediment of marine and
446 fluvial origin can be observed. This is reflected in the measured mass fractions of Zn, as well.
447 Sediment samples S_10 and S_11 with high amounts of Zn (879 mg kg^{-1} and 826 mg kg^{-1} Zn)
448 are rapidly diluted with marine sediment with significantly lower Zn mass fractions. This
449 phenomenon was studied in detail by Reese et al. (2019) using isotope-amount ratio analysis
450 of $n(^{87}\text{Sr})/n(^{86}\text{Sr})$, $n(^{143}\text{Nd})/n(^{144}\text{Nd})$ and multi-elemental mass fraction data. As no significant
451 change in isotopic composition of $\delta^{66}\text{Zn}/^{64}\text{Zn}_{\text{IRMM-3702}}$ could be observed for samples taken in
452 the Elbe River estuary, it can be assumed that the isotopic composition of Zn, is similar for
453 fluvial as well as for marine sediments in the investigated catchment area.

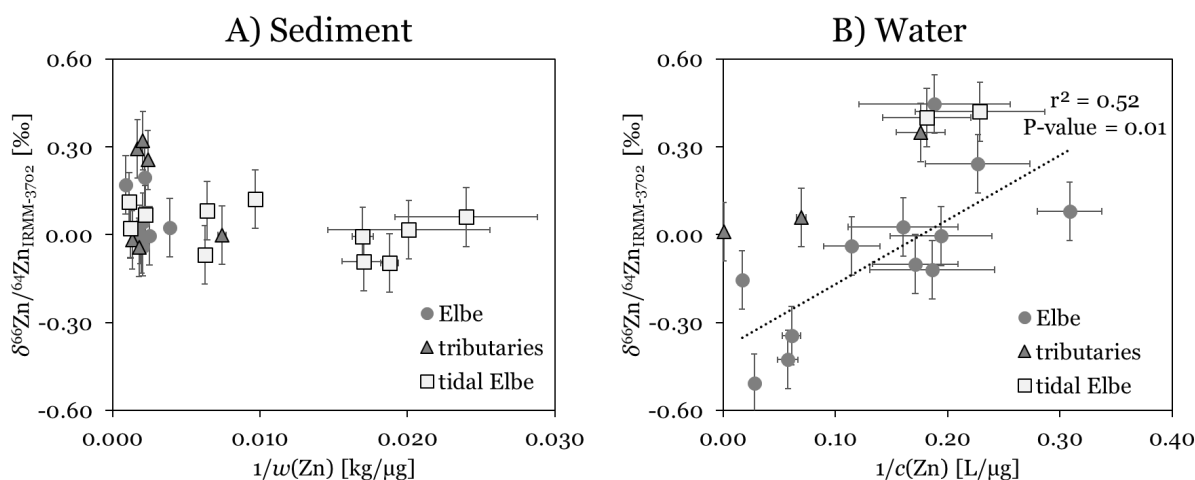
454 Three tributaries of the Elbe River, the Mulde ($\delta^{66}\text{Zn}/^{64}\text{Zn}_{\text{IRMM-3702}} 0.29 \text{ ‰} \pm 0.10 \text{ ‰}$, S_22 Tb.
455 Mulde, km 260), the Triebisch ($\delta^{66}\text{Zn}/^{64}\text{Zn}_{\text{IRMM-3702}} 0.32 \text{ ‰} \pm 0.10 \text{ ‰}$, S_27 Tb. Triebisch, km
456 82) and the Müglitz ($\delta^{66}\text{Zn}/^{64}\text{Zn}_{\text{IRMM-3702}} 0.26 \text{ ‰} \pm 0.10 \text{ ‰}$, S_30 Tb. Müglitz, km 39) are the
457 only samples with significantly heavier isotopic composition. As shown in Fig. 4A, no direct
458 linear correlation of the Zn isotopic composition and Zn mass fraction of sediment samples
459 could be observed.

460 Other studies reported heavier isotopic composition of sediment samples caused by
461 anthropogenic Zn emissions e.g. by Zn ore treatment plants (Araújo et al., 2017; Sivry et al.,
462 2008, Skierszkan et al., 2016). This is mainly due to the significantly heavier isotopic
463 composition of industrial tailings from Zn production relative to Zn ores, caused by the
464 production processes. In fact, the three tributaries rise in the nearby Ore Mountains, a region
465 in which mining activities started as early as in the Middle Ages. Especially during the 20th
466 century, the catchment of the Freiburger Mulde (as part of the Mulde River), was characterized
467 by Zn ore mining and processing of the ore leading to high, anthropogenic Zn amounts in water
468 and sediment of the Mulde River (Volland B.).

469 Another explanation may also lie in changes of bedrock geology (see Fig. 3) that may lead to
470 the heavier isotopic composition, as it is known for Zn bearing minerals featuring great
471 variability in Zn isotopic composition with reported $\delta^{66}\text{Zn}/^{64}\text{Zn}_{\text{IRMM-3702}}$ values of up to 1.10 ‰
472 (corresponding to $\delta^{66}\text{Zn}/^{64}\text{Zn}_{\text{JMC-Lyon}}$ value of 1.39 ‰) (Mondillo et al., 2018).
473 Overall our data indicates anthropogenic Zn sources to contribute to the total Zn load in the
474 tributaries.



476 **Fig. 3.** Surface geology of the Elbe River catchment within Germany (Rohstoffe, 2006)
477
478
479



480
 481 **Fig. 4.** A) $\delta^{66/64}\text{Zn}_{\text{IRMM-3702}}$ of sediment samples compared to inverse Zn mass fractions B)
 482 $\delta^{66/64}\text{Zn}_{\text{IRMM-3702}}$ of water samples compared to inverse dissolved Zn concentrations. The given
 483 trend line does not include values from tributaries and the tidal Elbe. Error bars correspond to
 484 $U(k=1)$ for isotopic data and to $U(k=2)$ for mass fractions and concentrations, respectively
 485 (if not visible U = smaller than spotsize)
 486

487 4.3 Isotopic signatures of water samples

488 Measured $\delta^{66}\text{Zn}/^{64}\text{Zn}_{\text{IRMM-3702}}$ of Elbe water samples had an average value of $0.02\text{‰} \pm 0.28\text{‰}$
 489 that is in accordance to the terrestrial background of $\delta^{66}\text{Zn}/^{64}\text{Zn}_{\text{IRMM-3702}}$ $0.0\text{‰} \pm 0.05\text{‰}$ (Chen
 490 et al., 2013). Although selected samples feature significantly higher, but also lower
 491 $\delta^{66}\text{Zn}/^{64}\text{Zn}_{\text{IRMM-3702}}$ values than the terrestrial background. In fact, a positive correlation
 492 between the Zn isotopic composition and the dissolved Zn concentration in the water phase
 493 might be possible, as shown in Fig. 4B. In case of the Elbe River generally lower concentrations
 494 of dissolved Zn are paired with heavier $\delta^{66}\text{Zn}/^{64}\text{Zn}_{\text{IRMM-3702}}$ values. An observation which has
 495 been described by Little et al. (2014) in a compilation of different water samples from various
 496 river systems.

497 Similar correlations were also observed for the isotopic systems of Cu and Mo (Vance et al.,
 498 2008, Archer and Vance, 2008), where isotopic fractionation processes are mainly caused by
 499 natural redox processes. Unlike Cu or Mo, Zn has only one oxidation state, neglecting
 500 fractionation processes related to redox reactions. Furthermore, lighter as well as heavier
 501 isotopic compositions of dissolved $\delta^{66}\text{Zn}/^{64}\text{Zn}$ than the lithogenic value have been reported in

502 literature (Little et al., 2014), therefore more complex biogeochemical fractionation processes
503 have to be taken into account.

504 A major source of Zn emissions into the environment are effluence of industrial tailings, which
505 potentially change the Zn isotopic composition of water and can therefore be used as a potential
506 tracer for anthropogenic Zn emissions. This raises the question of possible fractionation
507 processes between bedrock and water phase during weathering. In case of the oxidative
508 dissolution of sphalerite at laboratory conditions an initial increase in $\delta^{66}\text{Zn}/^{64}\text{Zn}_{\text{IRMM-3702}}$ of 0.2
509 ‰ in the dissolved fraction has been described. However, the observation of significant
510 isotopic fractionation vanished after dissolution of more than 1% of the mineral (Fernandez
511 and Borrok, 2009). Furthermore, analysis of dissolved $\delta^{66}\text{Zn}/^{64}\text{Zn}$ in waste rock drainage
512 waters varied little, with a $\delta^{66}\text{Zn}/^{64}\text{Zn}_{\text{IRMM-3702}}$ of $0.06 \text{ ‰} \pm 0.08 \text{ ‰}$. This value is in accordance
513 to the natural isotopic composition of bedrock (Matthies et al., 2014). Therefore, it seems
514 possible that natural fractionation between bedrock or mine tailings and dissolved Zn is
515 insignificant once a system reached steady state. Taken into account the significantly heavier
516 isotopic composition of some mine tailings ($\delta^{66}\text{Zn}/^{64}\text{Zn}_{\text{JMC-Lyon}}$ of up to 1.49 ‰, corresponding
517 to $\delta^{66}\text{Zn}/^{64}\text{Zn}_{\text{IRMM-3702}}$ of 1.20 ‰ (Sivry et al., 2008)) the isotopic composition of dissolved Zn
518 may be influenced by mine tailing effluent water.

519 **4.4 Potential influence of pH and SPM on isotope signatures of dissolved Zn**

520 A pronounced natural fractionation process leading to an isotopic composition enriched in
521 lighter dissolved Zn isotopes is described to be the sorption of preferably heavier isotopes to
522 suspended matter. A process that has been studied e.g. for the sorption of Zn to the surface of
523 iron oxides with a $(\Delta^{66}\text{Zn}/^{64}\text{Zn})_{\text{sorbed-aqueous}}$ of up to 0.53 ‰ (Juillot et al., 2008) and for the
524 sorption on the surface of kaolinite $(\Delta^{66}\text{Zn}/^{64}\text{Zn})_{\text{absorped-solution}}$ of up to 0.49 ‰ (Guinoiseau et
525 al., 2016). These sorption processes are described to be dependent on pH and ionic strength,
526 with potential larger fractionation at higher pH and higher ionic strength (Guinoiseau et al.,

2016, Bryan et al., 2015). Dissolved Zn may also be fractionated by the preferable sorption of heavy isotopes ($(\Delta^{66}\text{Zn}/^{64}\text{Zn})_{\text{sorbed-aqueous}}$ of up to 0.24 ‰) to humic acid, an analogue of organic matter (Jouvin et al., 2009).

Our data indicate potential fractionation processes of dissolved Zn dependent on the pH-value. As shown in Fig. 5, an increasing pH-value potentially leads to a lighter isotopic signature of dissolved Zn, thus heavier isotopes might be preferably removed from the water phase. Szykiewicz and Borrock (2016) previously described this process for water samples taken in the Rio Grande watershed, with a maximum of isotopic fractionation happening at pH-values between 8.0 and 8.5. This indicates that the pH-value plays an important role on natural fractionation of dissolved Zn not only for less anthropogenically impacted rivers like the Rio Grande, but also for anthropogenically impacted rivers like the Elbe.

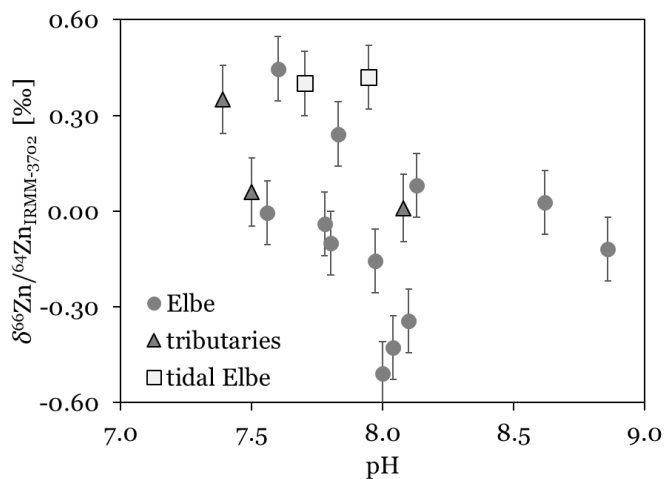


Fig. 5. $\delta^{66}\text{Zn}/^{64}\text{Zn}_{\text{IRMM-3702}}$ of water samples plotted versus the pH-value. Error bars correspond to U ($k = 1$) for isotopic data.

Nevertheless, natural processes might also lead to an enrichment of heavy Zn isotopes in the water phase. The preferable uptake of light Zn by organisms might represent another key factor of possible natural fractionation processes leading to a heavier isotopic composition of the water phase. This process is also thought to play an important role in the oceanographic mass balance of Zn, as dissolved Zn in the oceans is isotopically heavier ($\delta^{66}\text{Zn}/^{64}\text{Zn}_{\text{IRMM-3702}}$ of 0.21

548 ‰ corresponding to $\delta^{66}\text{Zn}/^{64}\text{Zn}_{\text{JMC-Lyon}}$ of 0.50 ‰,) than the riverine input of Zn (Little et al.,
549 2014). Experimental work on the uptake of Zn by marine diatom cells showed a preferable
550 uptake of light Zn by the cells, with a $\Delta^{66}\text{Zn}/^{64}\text{Zn}_{\text{cell-aqueous}}$ of up to -0.8 ‰ (John et al., 2007a).
551 Analysis of lake settling particles proved a significant isotope fractionation of $\delta^{66}\text{Zn}/^{64}\text{Zn}_{\text{IRMM-}}$
552 3702 $-0.95 \text{ ‰} \pm 0.08 \text{ ‰}$ (corresponding to $\delta^{66}\text{Zn}/^{64}\text{Zn}_{\text{JMC-Lyon}}$ $-0.66 \text{ ‰} \pm 0.08 \text{ ‰}$), caused by the
553 preferable uptake of lighter Zn isotopes by algae associated to the suspended particular matter
554 (SPM). The largest isotope fractionation was found during summer period with highest algae
555 production (Peel et al., 2009), a process likely to happen also for samples in this study, as
556 sampling was done during the high summer period. It should be mentioned that the degree of
557 possible isotopic fractionation for dissolved Zn in the water phase depends on the amount of
558 Zn taken up by algae. If this is insignificant in comparison to the amount of dissolved Zn in the
559 water phase, no changes in the isotopic composition of dissolved Zn will be observed.

560

561 **5. Summary and conclusion**

562 Stable Zn isotope abundance ratios and Zn concentrations/mass fractions were assessed in 19
563 water and 26 surface sediment samples from the German Elbe between the German/Czech
564 border and the German North Sea, including the main tributaries the Havel, the Saale and the
565 Mulde. Measured $\delta^{66}\text{Zn}/^{64}\text{Zn}_{\text{IRMM-3702}}$ values of the sediment samples are in good accordance
566 to the terrestrial background ($\delta^{66}\text{Zn}/^{64}\text{Zn}_{\text{IRMM-3702}}$ of $0.0 \text{ ‰} \pm 0.05 \text{ ‰}$), except for the tributaries
567 Mulde, Triebisch and Müglitz, which feature significantly heavier isotopic compositions.
568 Potential sources are discussed to be either of anthropogenic origin or caused by changes in
569 bedrock geology. $\delta^{66}\text{Zn}/^{64}\text{Zn}_{\text{IRMM-3702}}$ values of the water samples showed larger variability
570 ($\delta^{66}\text{Zn}/^{64}\text{Zn}_{\text{IRMM-3702}}$ ranging from -0.51 ‰ to 0.45 ‰) and a potential linear correlation with
571 dissolved Zn concentrations. Generally lower concentrations of dissolved Zn are paired with
572 heavier $\delta^{66}\text{Zn}/^{64}\text{Zn}_{\text{IRMM-3702}}$ values and vice versa, indicating complex fractionation processes

573 of dissolved Zn even for an anthropogenically impacted river like the Elbe. Furthermore, the
574 pH-value may play another important role for natural fractionation processes. Our results
575 indicate that even though Zn isotope abundance ratio analysis has been successfully applied in
576 order to trace anthropogenic Zn emissions, natural fractionation processes play an important
577 role in the biogeochemistry of Zn, making it challenging to distinctly trace anthropogenic Zn
578 emissions in large river systems. Until today, only few publications have reported Zn isotopic
579 composition in river systems at a large regional scale. Therefore, our work will help to better
580 understand biogeochemical fractionation processes, as well as possible anthropogenic
581 influences on the isotopic composition of Zn in such systems. However, this study does not
582 provide any data regarding the seasonal changes of natural fractionation processes, especially
583 for dissolved Zn. Future studies should also include the analysis of SPM, as SPM reflects an
584 important link between the sediment and the dissolved Zn of the water phase. This study also
585 demonstrates once more that profound knowledge of the biogeochemical fractionation
586 processes are a prerequisite for correct data interpretation, processes that are not fully
587 understood yet.

588 **Acknowledgements**

589 The authors would like to thank Thomas Prohaska for his scientific input. Furthermore, we
590 would like to thank Andrea Lapschies for their support in the lab. Tristan Zimmermann would
591 like to thank the Commission on Isotopic Abundances and Atomic Weights for financial
592 support from project 2011-026-1-200 for travel expenses to the University of Calgary.

593

594 **Competing interests declaration**

595 The authors have no competing interests to declare.

596 **Funding**

597 This research did receive funding from the Commission on Isotopic Abundances and Atomic
598 Weights. M. E. Wieser is supported by a Discovery Grant from the Natural Sciences and
599 Engineering Research Council of Canada. A. F. Mohamed received support from the Canadian
600 Bureau for International Education.

601 **References**

- 602
603 Ackermann F, Bergmann H, Schleichert U. Monitoring of heavy metals in coastal and estuarine
604 sediments - a question of grain-size: <20 μm versus <60 μm . *Environmental*
605 *Technology Letters* 1983; 4: 317-328.
- 606 Araújo DF, Boaventura GR, Machado W, Viers J, Weiss D, Patchineelam SR, et al. Tracing of
607 anthropogenic zinc sources in coastal environments using stable isotope composition.
608 *Chemical Geology* 2017; 449: 226-235.
- 609 Archer C, Andersen AB, Cloquet C, Conway TM, Dong S, Ellwood M, Moore R, Nelson J,
610 Rehkämper M, Rouxel O, Samanta M; Shin KC, Sohrin Y, Takano S, Wasylenski L.
611 Inter-calibration of a proposed new primary reference standard AA-ETH Zn for zinc
612 isotopic analysis. *Journal of Analytical Atomic Spectrometry* 2017; 32: 415-419.
- 613 Archer C, Vance D. Mass discrimination correction in multiple-collector plasma source mass
614 spectrometry: an example using Cu and Zn isotopes. *Journal of Analytical Atomic*
615 *Spectrometry* 2004; 19: 656-665.
- 616 Archer C, Vance D. The isotopic signature of the global riverine molybdenum flux and anoxia
617 in the ancient oceans. *Nature Geoscience* 2008; 1: 597-600.
- 618 Arnold T, Schonbachler M, Rehkämper M, Dong SF, Zhao FJ, Kirk GJD, et al. Measurement
619 of zinc stable isotope ratios in biogeochemical matrices by double-spike MC-ICPMS
620 and determination of the isotope ratio pool available for plants from soil. *Analytical and*
621 *Bioanalytical Chemistry* 2010; 398: 3115-3125.
- 622 ATV-DVWK. Die Elbe und ihre Nebenflüsse Belastung, Trends, Bewertung, Perspektiven
623 2000.
- 624 Bermin J, Vance D, Archer C, Statham PJ. The determination of the isotopic composition of
625 Cu and Zn in seawater. *Chemical Geology* 2006; 226: 280-297.
- 626 Blix R, Vonubisch H, Wickman FE. A Search for Variations in the Relative Abundance of the
627 Zinc Isotopes in Nature. *Geochimica Et Cosmochimica Acta* 1957; 11: 162-164.
- 628 Bohlich MJ, Strotmann T. The Elbe Estuary. *Die Küste* 2008: 288-306.
- 629 Brand WA, Coplen TB, Vogl J, Rosner M, Prohaska T. Assessment of international reference
630 materials for isotope-ratio analysis (IUPAC Technical Report). *Pure and Applied*
631 *Chemistry* 2014; 86: 425-467.

- 632 Brase L, Bange HW, Lendt R, Sanders T, Dähnke K. High Resolution Measurements of Nitrous
633 Oxide (N₂O) in the Elbe Estuary. *Frontiers in Marine Science* 2017; 4:162.
- 634 Bryan AL, Dong SF, Wilkes EB, Wasylenki LE. Zinc isotope fractionation during adsorption
635 onto Mn oxyhydroxide at low and high ionic strength. *Geochimica et Cosmochimica*
636 *Acta* 2015; 157: 182-197.
- 637 Chen H, Savage PS, Teng F-Z, Helz RT, Moynier F. Zinc isotope fractionation during
638 magmatic differentiation and the isotopic composition of the bulk Earth. *Earth and*
639 *Planetary Science Letters* 2013; 369-370: 34-42.
- 640 Chen JB, Gaillardet J, Louvat P. Zinc isotopes in the Seine River waters, France: A probe of
641 anthropogenic contamination. *Environmental Science & Technology* 2008; 42: 6494-
642 6501.
- 643 Chen JB, Gaillardet J, Louvat P, Huon S. Zn isotopes in the suspended load of the Seine River,
644 France: Isotopic variations and source determination. *Geochimica Et Cosmochimica*
645 *Acta* 2009; 73: 4060-4076.
- 646 Fernandez A, Borrok DM. Fractionation of Cu, Fe, and Zn isotopes during the oxidative
647 weathering of sulfide-rich rocks. *Chemical Geology* 2009; 264: 1-12.
- 648 Gonzalez RO, Strekopytov S, Amato F, Querol X, Reche C, Weiss D. New Insights from Zinc
649 and Copper Isotopic Compositions into the Sources of Atmospheric Particulate Matter
650 from Two Major European Cities. *Environmental Science & Technology* 2016; 50:
651 9816-9824.
- 652 Gonzalez RO, Weiss D. Zinc Isotope Variability in Three Coal-Fired Power Plants: A
653 Predictive Model for Determining Isotopic Fractionation during Combustion.
654 *Environmental Science & Technology* 2015; 49: 12560-12567.
- 655 Guinoiseau D, Gélabert A, Moureau J, Louvat P, Benedetti MF. Zn Isotope Fractionation
656 during Sorption onto Kaolinite. *Environmental Science & Technology* 2016; 50: 1844-
657 1852.
- 658 IKSE Internationale Kommission zur Schutz der Elbe. Hydrologische Auswertung der
659 Niedrigwassersituation 2015 im Einzugsgebiet der Elbe. 2017.
- 660 John SG, Geis RW, Saito MA, Boyle EA. Zinc isotope fractionation during high-affinity and
661 low-affinity zinc transport by the marine diatom *Thalassiosira oceanica*. *Limnology and*
662 *Oceanography* 2007a; 52: 2710-2714.
- 663 John SG, Park JG, Zhan ZT, Boyle EA. The isotopic composition of some common forms of
664 anthropogenic zinc. *Chemical Geology* 2007b; 245: 61-69.
- 665 Jouvin D, Louvat P, Juillot F, Maréchal CN, Benedetti MF. Zinc Isotopic Fractionation: Why
666 Organic Matters. *Environmental Science & Technology* 2009; 43: 5747-5754.
- 667 Juillot F, Maréchal C, Ponthieu M, Cacaly S, Morin G, Benedetti M, et al. Zn isotopic
668 fractionation caused by sorption on goethite and 2-Lines ferrihydrite. *Geochimica et*
669 *Cosmochimica Acta* 2008; 72: 4886-4900.
- 670 Kragten J. Tutorial review. Calculating standard deviations and confidence intervals with a
671 universally applicable spreadsheet technique. *Analyst* 1994; 119: 2161-2165.
- 672 LAWA Länderarbeitsgemeinschaft Wasser. Zielvorgaben zum Schutz oberirdischer
673 Binnengewässer, Band II. 1998.

- 674 Little SH, Vance D, Walker-Brown C, Landing WM. The oceanic mass balance of copper and
675 zinc isotopes, investigated by analysis of their inputs, and outputs to ferromanganese
676 oxide sediments. *Geochimica et Cosmochimica Acta* 2014; 125: 673-693.
- 677 Maréchal CN, Nicolas E, Douchet C, Albarède F. Abundance of zinc isotopes as a marine
678 biogeochemical tracer. *Geochemistry Geophysics Geosystems* 2000; 1.
- 679 Maréchal CN, Telouk P, Albarède F. Precise analysis of copper and zinc isotopic compositions
680 by plasma-source mass spectrometry. *Chemical Geology* 1999; 156: 251-273.
- 681 Matthies R, Sinclair SA, Blowes DW. The zinc stable isotope signature of waste rock drainage
682 in the Canadian permafrost region. *Applied Geochemistry* 2014; 48: 53-57.
- 683 Mattielli N, Petit JCJ, Deboudt K, Flament P, Perdrix E, Taillez A, et al. Zn isotope study of
684 atmospheric emissions and dry depositions within a 5 km radius of a Pb-Zn refinery.
685 *Atmospheric Environment* 2009; 43: 1265-1272.
- 686 Moeller K, Schoenberg R, Pedersen RB, Weiss D, Dong SF. Calibration of the New Certified
687 Reference Materials ERM-AE633 and ERM-AE647 for Copper and IRMM-3702 for
688 Zinc Isotope Amount Ratio Determinations. *Geostandards and Geoanalytical Research*
689 2012; 36: 177-199.
- 690 Mondillo N, Wilkinson J, Boni M, Weiss D, Mathur R. A global assessment of Zn isotope
691 fractionation in secondary Zn minerals from sulfide and non-sulfide ore deposits and
692 model for fractionation control. *Chemical Geology* 2018; 500:182-193.
- 693 Moore RET, Lerner F, Coles BJ, Rehkamper M. High Precision Zinc Stable Isotope
694 Measurement of Certified Biological Reference Materials Using the Double Spike
695 Technique and Multiple Collector-ICP-MS. *Analytical and Bioanalytical Chemistry*
696 2017; 409: 2941-2950.
- 697 Peel K, Weiss D, Sigg L. Zinc isotope composition of settling particles as a proxy for
698 biogeochemical processes in lakes: Insights from the eutrophic Lake Greifen,
699 Switzerland. *Limnology and Oceanography* 2009; 54:1699-1708.
- 700 Petit JCJ, de Jong J, Chou L, Mattielli N. Development of Cu and Zn isotope MC-ICP-MS
701 measurements: Application to suspended particulate matter and sediments from the
702 Scheldt estuary. *Geostandards and Geoanalytical Research* 2008; 32: 149-166.
- 703 Pichat S, Douchet C, Albarède F. Zinc isotope variations in deep-sea carbonates from the
704 eastern equatorial Pacific over the last 175 ka. *Earth and Planetary Science Letters*
705 2003; 210: 167-178.
- 706 Ponzevera E, Quérel CR, Berglund M, Taylor PDP, Evans P, Loss RD, et al. Mass
707 discrimination during MC-ICPMS isotopic ratio measurements: Investigation by means
708 of synthetic isotopic mixtures (IRMM-007 series) and application to the calibration of
709 natural-like zinc materials (including IRMM-3702 and IRMM-651). *Journal of the*
710 *American Society for Mass Spectrometry* 2006; 17: 1412-1427.
- 711 Prange A, Bössow E, Erbslöh B, Jablonski R, Jantzen E, Kause P, et al. Grafische Darstellung
712 der Längsprofile - Filtarte, Schwebstoffe, Sedimente -. Erfassung und Beurteilung der
713 Belastung der Elbe mit Schafstoffe. GKSS-Forschungszentrum Geesthacht GmbH,
714 Geesthacht, 2001.
- 715 Prange A, Bössow E, Erbslöh B, Jablonski R, Jantzen E, Krause P, et al. Zusammenfassende
716 Aus-und Bewertung der Längsprofiluntersuchungen in der Elbe. Institut für

717 Physikalische und Chemische Analytik-GKSS-Forschungszentrum Geesthacht GmbH,
718 Geesthacht 1997.

719 Reese A, Zimmermann T, Pröfrock D, Irrgeher J. Extreme spatial variation of Sr, Nd and Pb
720 isotopic signatures and 48 element mass fractions in surface sediment of the Elbe River
721 Estuary - Suitable tracers for processes in dynamic environments? *Science of The Total*
722 *Environment* 2019; 668: 512-523.

723 Rohstoffe BfGu. Geological Map of Germany 1:1,000,000 (GK1000), 2006.

724 Sivry Y, Riotte J, Sonke JE, Audry S, Schafer J, Viers J, et al. Zn isotopes as tracers of
725 anthropogenic pollution from Zn-ore smelters The Riou Mort-Lot River system.
726 *Chemical Geology* 2008; 255: 295-304.

727 Skierszkan E K, Mayer K U, Weis D, Beckie R D, Molybdenum and zinc stable isotope
728 variation in mining waste rock drainage and waste rock at the Antamina mine, Peru.
729 *Science of The Total Environment* 2016; 550:103-113.

730 Sühling R, Busch F, Fricke N, Kötke D, Wolschke H, Ebinghaus R. Distribution of brominated
731 flame retardants and dechloranes between sediments and benthic fish - A comparison
732 of a freshwater and marine habitat. Vol 542, 2015.

733 U.S. Geological Survey . Mineral commodity summaries 2017 : U .S. Geological Survey. 2017.
734 [http s:// doi.org/10.3133/70180](http://doi.org/10.3133/70180)

735 Szykiewicz A, Borrok DM. Isotope variations of dissolved Zn in the Rio Grande watershed,
736 USA: The role of adsorption on Zn isotope composition. *Earth and Planetary Science*
737 *Letters* 2016; 433: 293-302.

738 Thapalia A, Borrok DM, Van Metre PC, Wilson J. Zinc Isotopic Signatures in Eight Lake
739 Sediment Cores from Across the United States. *Environmental Science & Technology*
740 2015; 49: 132-140.

741 Vance D, Archer C, Bermin J, Perkins J, Statham PJ, Lohan MC, et al. The copper isotope
742 geochemistry of rivers and the oceans. *Earth and Planetary Science Letters* 2008; 274:
743 204-213.

744 Vink R., Behrendt H., Salomons W., Development of the heavy metal pollution trends in
745 several Europaen Rivers: An analysis of point and diffuse sources. *Water Science and*
746 *Technology* 1999; 12: 215-223.

747 Voland B. KA. Geogene und anthropogene Quellen der Schwermetallbelastung von
748 Fließgewässern des Erzgebirges. *DVGW Schriftreihe Wasser*; 109: 117-137.

749 Weiss DJ, Mason TFD, Zhao FJ, Kirk GJD, Coles BJ, Horstwood MSA. Isotopic
750 discrimination of zinc in higher plants. *New Phytologist* 2005; 165: 703-710.

751 Voitke P, Wellnitz J, Helm D, Kube P, Lepom P, Litheraty P. Analysis and assessment of
752 heavy metal pollution in suspended solids and sediments of the river Danube.
753 *Chemosphere* 2003; 51:633-642.

754